SEMARAK ILMU PUBLISHING

Journal of Advanced Research in Applied Sciences and Engineering Technology

Journal homepage: https://semarakilmu.com.my/journals/index.php/applied_sciences_eng_tech/index
ISSN: 2462-1943

Comparison of Higher-Order Beam Theory and First-Order Beam Theory Models on FGM Beam Element for Static Analysis

Anastasya Martina[1], Irwan Katili[1,*], Susilo Widyatmoko[1]

[1] Department of Civil Engineering, Civil Engineering Faculty, University of Indonesia, 16424 Depok, Indonesia

ARTICLE INFO

Article history:
Received 3 November 2023
Received in revised form 29 July 2024
Accepted 29 August 2024
Available online 20 September 2024

Keywords:
HOBT; Two independent variables; Finite element method; 3rd degree polynomial

ABSTRACT

HOBT-Higher Order Beam Theory is the developing theory in the Finite Element Method (FEM), which considers the higher-order variation of transverse shear strain; therefore, the shear correction factor is not required. This paper uses beam elements and implements them to higher order beam theory developed by Vo *et al.,* with two independent variables of bending and shear displacement, using third-order polynomial functions. This paper shows the contribution of the shear strain part as one of the independent variables. Static analyses are presented to obtain a comparative result with the First Order Beam Theory (FOBT) application on the imposition of different boundary conditions to ensure reliable results.

1. Introduction

Nowadays, advanced technology use Functionally Graded Materials (FGMs), whose structural properties are varied along their volume to meet an expected function and have been applied in the structural industry [1-3]; however, there is a challenge for FGM (Functionally Graded Material) as structural components in extremely high-temperature environments to eliminate the shear stress concentrations both upper and bottom of the element with the simplicity of the element consideration [4,5]. In FEA (Finite Element Analysis), the simulation solution depends on the number of degrees of freedom (DOF) of the system to be analysed as the minimum number of independent coordinates that can specify the position of the system completely [10]. The simplest model in FEA is Classical Beam Theory (CBT). CBT delivers satisfactory results of static and free vibration analysis for thin beams, on the other hand for thick beams where the transverse shear effect exists. When it implements to thick beam the static result is undervalued and natural frequency is overestimated. First Order Beam Theory (FOBT) which also known as Timoshenko beam theory take into account the effects of shear deformation, Timoshenko proposed a further improvement of the beam theory to accommodate the thick beam analysis, but this theory suffers from a phenomenon called shear locking when analysing thin beams. Timoshenko theory needs special treatment to prevent shear

* *Corresponding author.*
E-mail address: irwan.katili@ui.ac.id

https://doi.org/10.37934/araset.53.2.5773

locking problem [4-6]. Another FOBT theory as modification of Timoshenko Beam Theory using unified integrated (UI) approach has been proposed in reference [7-10]. UI approach has been developed by Katili, who presented the development of a beam element without shear locking problem called UI (Unified and Integrated) method using the C2 Hermite polynomial expansion of the 5th degree for bending displacement w_b [11-13]. Based on this, Katili developed a more efficient FOBT with two-node 3 DOFs FGM beam element as a simplification of previous studies [14]. Both UI Method and UI Simplified use shear correction factor $k = \frac{5}{6}$.

The studies on the higher-order beam theory and its application to FGM, have received much research attention over recent years which are taken from previous studies [17-24]. Higher-Order Beam Theory (HOBT) have been proposed to avoid the use of a shear correction factor and have a better prediction of response of FGM beams. The Higher Order theory developed by Vo *et al.,* [21] provides two independent variables assumption of the bending and shear displacement variables, where the shear displacement does not depend on the derivative of the bending displacement formulation. This study uses the following assumptions:

i. axial and transverse displacements are divided into bending and shear components
ii. the axial displacement bending components are similar to those given by CBT (Classical Beam Theory
iii. the shear component obtained from higher order theoretical calculations given by Reddy with reference [25-29].

In this paper, those three are developed with Reddy assumption of constant transverse displacement and higher order axial displacement through the depth of the beam. The elements in this study use Finite Element Method with third-degree of polynomial Hermitian functions for the bending w_b and shear w_s displacement contribution, then for slope displacement θ_b and θ_s are the first derivative of w_b and w_s, This research assumes the unlinking of the two bending and shear variables and develops a formulation from Vo, *et al.,* [21]. The proposed theories satisfy condition where shear stress will be at a maximum value at the centre of the beam and will be zero at the top and bottom of the beam, thus a shear correction factor is not required. Furthermore, Comparison several numerical results of different boundary conditions and implementation of others two UI theories to provide validation of the static analysis results.

The organization of the paper is as follows. After the introduction, the Higher-Order Beam Theory for FGM beam and First-Order Beam Theory are presented in Section 2. Section 3 presents the numerical results of Static Analysis and the comparison with another method and followed by conclusions in Section 4.

2. FGM Beam Theory

Consider a beam with length L and rectangular cross-section $b \times h$, with b as the width and h being the height. The x-, y-, and z-coordinates are taken along the length, width, and height of the beam. The formulation is limited to linear elastic material behaviour.

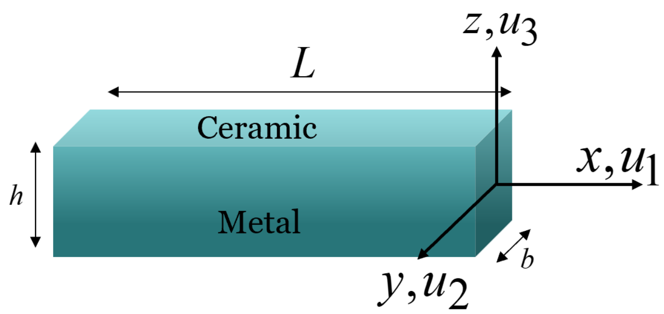

Fig. 1. Geometry and Coordinate systems of FGM Beam

2.1 Higher Order Beam Theory

Considering the arbitrary displacement field is given by the following expression:

$$u_1(x,z,t) = u_a(x,t) - z\frac{dw_b}{dx} - f(z)\frac{dw_s}{dx} \tag{1}$$

$$u_2(x,z,t) = 0 \tag{2}$$

$$u_3(x,z,t) = w_b(x,t) + w_s(x,t) \tag{3}$$

Where u_a is the axial displacement in mid of the beam, w_b and w_s are the bending and shear components of transversal displacement in the centre of the beam. $f(z)$ is a shape function expression of transverse shear stress distribution along the thickness of the beam based on Reddy's assumption [25], which is expressed in the following equation:

$$f(z) = \frac{4z^3}{3h^2}; g(z) = 1 - \frac{df}{dz} = 1 - \frac{4z^2}{h^2} \tag{4}$$

By substituting Eq. (4) to Eq. (1), The normal strain is:

$$\varepsilon_x = \frac{du_1}{dx} = \frac{du_a}{dx} - z\frac{d^2w_b}{dx^2} - f(z)\frac{d^2w_s}{dx^2}; \tag{5}$$

The normal stress-normal strain relationship is:

$$\sigma_x = E(z)\varepsilon_x \tag{6}$$

$$\sigma_x = E(z)\left(\frac{du_a}{dx} - z\frac{d^2w_b}{dx^2} - f(z)\frac{d^2w_s}{dx^2}\right); \tag{7}$$

The transverse shear strain along the beam is:

$$\gamma_{xz} = \frac{du_1}{dz} + \frac{du_3}{dx} = \left(1 - \frac{df(z)}{dz}\right)\frac{dw_s}{dx} = g(z)\left(\frac{dw_s}{dx}\right); \tag{8}$$

The shear modulus and the shear stress-shear strain relationship is:

$$G(z) = \frac{E(z)}{2(1+v(z))}; \tag{9}$$

$$\sigma_{xz} = G(z)\left(g(z)\frac{dw_s}{dx}\right) \tag{10}$$

Where $E(z)$ is the young elastic modulus, $G(z)$ is the shear modulus, and $v(z)$ which is Poisson's ratio along the thickness.

Hamilton Principle is used for the equation of motion. The analytical form of the equation is given by:

$$0 = \int_{t_2}^{t_2} (\delta U + \delta V - \delta K)dt \tag{11}$$

$$\delta U = \int_0^L \int_A \left(\sigma_x \delta\varepsilon_x + \sigma_{xz}\delta\gamma_{xz}\right) dAdx; \tag{12}$$

$$\delta V = -\int_0^L f_0 \delta(w_b + w_s)dx \tag{13}$$

δU is the virtual variation of strain energy, δV is the virtual variation of potential energy and δK is the virtual variation of Kinetic Energy. This paper only considers the static analysis therefore $\delta K = 0$

The variation of strain energy is expressed in:

$$\partial U = \int_0^L \int_A \left(\sigma_x \delta\varepsilon_x + \sigma_{xz}\delta\gamma_{xz}\right) dA\ dx; \tag{14}$$

The axial strain e of the beam axis and curvature χ at any point *x* along the beam, transverse shear strain γ, bending rotation θ_b and shear rotation θ_s are given by:

$$\chi^b(x) = -\frac{d^2 w_b(x)}{dx^2}; \tag{15}$$

$$\chi^s(x) = -\frac{d^2 w_s(x)}{dx^2}; \tag{16}$$

$$e(x) = \frac{du_a(x)}{dx}; \tag{17}$$

$$\gamma_{xz} = g(z)\frac{dw_s(x)}{dx}; \tag{18}$$

$$\theta_b = \frac{dw_b(x)}{dx} \tag{19}$$

$$\theta_s = \frac{dw_s(x)}{dx} \tag{20}$$

FGM, in this theory, is composite material graded from ceramic to metal. The material properties of the FGM beam are assumed to vary along the thickness of the beam based on the power law from reference [21].

$$E(z) = E_m + (E_c - E_m)V_c; \tag{21}$$

$$\rho(z) = \rho_m + (\rho_c - \rho_m)V_c; \tag{22}$$

$$V_c = \left(\frac{1}{2} + \frac{z}{h}\right)^p; V_m = 1 - V_c \tag{23}$$

Where P denotes the effectiveness of material properties such as young modulus E, Poisson's ratio v, and mass density ρ. Subscripts *m* and *c* indicate the type of material metal and ceramic respectively; and p is the powerlaw index for volume fraction gradation identification. Figure 2 illustrates the variation of V_c along the beam thickness with different *p*. A value of $p = 0$ indicates full ceramic, and $p = \infty$ is full metal.

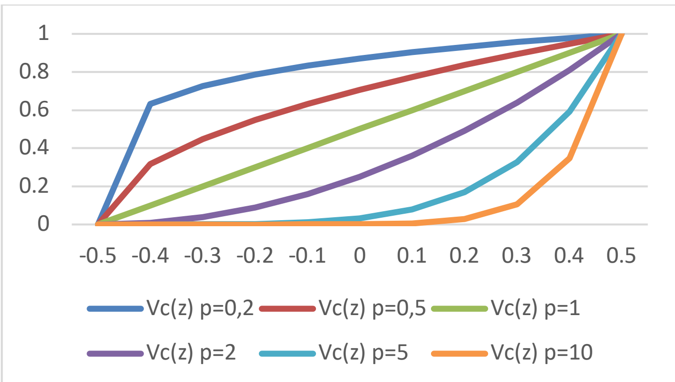

Fig. 2. V_c variation along the thickness of the beam with different powerlaw index

After substitution of Eq. (4) to Eq. (10) to Eq. (12), then stress resultant expression are given by:

Stress Resultant Axial Force:

$$N = D_a e(x) - D_{ab}\chi^b(x) - D_{as}\chi^s(x) \tag{24}$$

$$D_a = b\int_{-h/2}^{h/2} E(z)dz \tag{25}$$

$$D_{ab} = b\int_{-h/2}^{h/2} zE(z)dz \tag{26}$$

$$D_{as} = b\int_{-h/2}^{h/2} f(z)E(z)dz$$

Stress resultant Bending Moment:

$$M_b = D_{ab}e(x) - D_{bb}\chi^b(x) - D_{bs}\chi^s(x) \tag{27}$$

$$D_{bb} = b\int_{-h/2}^{h/2} z^2E(z)dz \tag{28}$$

$$D_{bs} = b\int_{-h/2}^{h/2} zf(z)E(z)dz \tag{29}$$

Stress resultant of shear force:

$$Q = D_s\gamma(x) \tag{30}$$

$$D_s = b\int_{-h/2}^{h/2} g^2(z)G(z)dz \tag{31}$$

Stress resultant Shear Moment:

$$M_s = D_{as}e(x) - D_{bs}\chi^b(x) - D_{ss}\chi^s(x) \tag{32}$$

$$D_{as} = b\int_{-h/2}^{h/2} f(z)E(z)dz \tag{33}$$

$$D_{bs} = b\int_{-h/2}^{h/2} zf(z)E(z)dz \tag{34}$$

$$D_{ss} = b \int_{-h/2}^{h/2} f^2(z) E(z) dz \tag{35}$$

By integrating Eq. (37) to Eq. (42), The classical principle of strain energy takes the form:

$$\Pi_{\text{int}} = \Pi_{\text{int}}^{a} + \Pi_{\text{int}}^{b} + \Pi_{\text{int}}^{s} + \Pi_{\text{int}}^{ab} + \Pi_{\text{int}}^{as} + \Pi_{\text{int}}^{bs} \tag{36}$$

Where:
Axial Energy :

$$\Pi_{\text{int}}^{a} = \frac{1}{2} D_a \int_0^L e^2 dx; \tag{37}$$

Bending Energy :

$$\Pi_{\text{int}}^{b} = \frac{1}{2} D_{bb} \int_0^L (\chi^b)^2 dx + \frac{1}{2} D_{ss} \int_0^L (\chi^s)^2 dx; \tag{38}$$

Shear Energy :

$$\Pi_{\text{int}}^{s} = \frac{1}{2} D_s \int_0^L \gamma^2 dx; \tag{39}$$

Axial-Bending Coupling Energy:

$$\Pi_{\text{int}}^{ab} = -\frac{1}{2} D_{ab} \int_0^L e\chi^b dx - \frac{1}{2} D_{ab} \int_0^L \chi^b e dx; \tag{40}$$

Axial-Shear Coupling Energy:

$$\Pi_{\text{int}}^{as} = -\frac{1}{2} D_{as} \int_0^L e\chi^s dx - \frac{1}{2} D_{as} \int_0^L \chi^s e dx; \tag{41}$$

Bending-Shear Coupling Energy:

$$\Pi_{\text{int}}^{bs} = -\frac{1}{2} D_{bs} \int_0^L \chi^b \chi^s dx - \frac{1}{2} D_{bs} \int_0^L \chi^s \chi^b dx; \tag{42}$$

2.2 HOBT Element

Figure 3 shown the 2-node beam is formulated in 5 DOFs ($u_a, w_b, \theta_b, w_s, \theta_s$), so there are 10 DOFs in one element. There are two unknown variables in the HOBT element equation. Those are the bending deformation which is defined by a 3rd-degree polynomial expansion, and the shear displacement which is approximated with the same 3rd-degree polynomial equation. The rotation function is the first derivative of its deformation. The bending displacement w_b and bending slope θ_b must be continuous across the elements in order to have a conforming finite element method, the cubic shape function are required.

Fig. 3. Degree of Freedom Beam Element

3rd degree Polynomial based shape function is used:

$$w_b = w_s = \langle 1 \quad x \quad x^2 \quad x^3 \rangle \begin{Bmatrix} a_1 \\ a_2 \\ a_3 \\ a_4 \end{Bmatrix} \tag{43}$$

$$w_b = \langle P_b \rangle \{a_n\} \tag{44}$$

$$w_s = \langle P_s \rangle \{a_n\} \tag{45}$$

Where $\{a_n\}^T = \{a_1 \quad a_2 \quad a_3 \quad a_4\}^T$

Substituting Eq. (43) to Eq. (19) and Eq. (20), we obtain the bending and shear rotation as follows:

$$\theta_b = \theta_s = \langle 0 \quad 1 \quad 2x \quad 3x^2 \rangle \begin{Bmatrix} a_1 \\ a_2 \\ a_3 \\ a_4 \end{Bmatrix} \tag{46}$$

$$\theta_b = \langle P'_b \rangle \{a_n\} \tag{47}$$

$$\theta_s = \langle P'_s \rangle \{a_n\} \tag{48}$$

By using the standard procedure of the finite element method, the shape function for the HOBT element in Figure 4 is:

$$N_{w_{b1}} = N_{w_{s1}} = \frac{(L-x)^2 (L+2x)}{L^3} \tag{49}$$

$$N_{\theta_{b1}} = N_{\theta_{s1}} = \frac{x(L-x)^2}{L^2} \tag{50}$$

$$N_{w_{b2}} = N_{w_{s2}} = \frac{x^2 (3L-2x)}{L^3}$$
(51)

$$N_{\theta_{b2}} = N_{\theta_{s2}} = -\frac{x^2 (L-x)}{L^2} \tag{52}$$

So, the graph of shape function becomes:

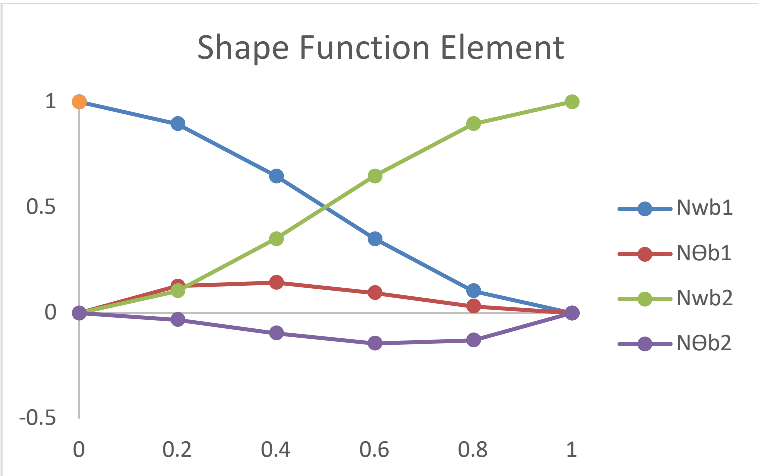

Fig. 4. Shape Function Bending and Shear of HOBT element

Then, by substituting Eq. (45) to Eq. (48) to Eq. (43) we obtain the bending and shear displacement with below formula.

$$w_b = \left\langle N_{w_{b1}} \quad N_{\theta_{b1}} \quad N_{w_{b2}} \quad N_{\theta_{b2}} \right\rangle \begin{Bmatrix} w_{b_1} \\ \theta_{b_1} \\ w_{b_2} \\ \theta_{b_2} \end{Bmatrix} \tag{53}$$

$$w_s = \left\langle N_{w_{s1}} \quad N_{\theta_{s1}} \quad N_{w_{s2}} \quad N_{\theta_{s2}} \right\rangle \begin{Bmatrix} w_{s_1} \\ \theta_{s_1} \\ w_{s_2} \\ \theta_{s_2} \end{Bmatrix} \tag{54}$$

Linear Polynomial is chosen for axial displacement, and the shape function of axial displacement is expressed below:

$$u_a = \left\langle N_{u_{a1}} \quad N_{u_{a2}} \right\rangle \begin{Bmatrix} u_{a_1} \\ u_{a_2} \end{Bmatrix} \tag{55}$$

$$N_{u_{a1}} = \left(\frac{L-x}{L} \right) \; ; \; N_{u_{a2}} = \left(\frac{x}{L} \right) \tag{56}$$

Substituting Eq. (55) to Eq. (17), we obtain the axial strain :

$$e = \left\langle B_{u_a} \right\rangle \{u_n\}; \tag{57}$$

Where the axial strain matrix B_{u_a} is:

$$\left\langle B_{u_a} \right\rangle = \left\langle -\frac{1}{L} \quad 0 \quad 0 \quad 0 \quad 0 \quad \frac{1}{L} \quad 0 \quad 0 \quad 0 \quad 0 \right\rangle \tag{58}$$

Substituting Eq. (53) to Eq. (15) gives curvature:

$$\chi = \left\langle B_b \right\rangle \{u_n\} \tag{59}$$

Where the bending strain matrix B_b is:

$$\left\langle B_b \right\rangle = \left\langle 0 \quad \left(\frac{2(L+2x)}{L^3} - \frac{4(2L-2x)}{L^3} \right) \quad \left(\frac{2x}{L^2} - \frac{2(2L-2x)}{L^2} \right) \quad 0 \quad 0 \quad 0 \quad \left(\frac{2(3L-2x)}{L^3} - \frac{8x}{L^3} \right) \quad \left(\frac{4x}{L^2} - \frac{2(L-x)}{L^2} \right) \quad 0 \quad 0 \right\rangle \tag{60}$$

Substituting Eq. (54) to Eq. (18) gives the shear strain:

$$\gamma = \left\langle B_s \right\rangle \{u_n\} \tag{61}$$

Where the shear strain matrix B_s is:

$$\left\langle B_s \right\rangle = \left\langle 0 \quad 0 \quad 0 \quad \left(\frac{2(L+2x)}{L^3} - \frac{4(2L-2x)}{L^3} \right) \quad \left(\frac{2x}{L^2} - \frac{2(2L-2x)}{L^2} \right) \quad 0 \quad 0 \quad 0 \quad \left(\frac{2(3L-2x)}{L^3} - \frac{8x}{L^3} \right) \quad \left(\frac{4x}{L^2} - \frac{2(L-x)}{L^2} \right) \right\rangle \tag{62}$$

By substituting Eq. (57) to Eq. (62) to Eq. (36), gives:
Axial Energy :

$$\Pi_{\text{int}}^{a} = \frac{1}{2}\langle u_n \rangle [K_a] \{u_n\} \tag{63}$$

Bending Energy :

$$\Pi_{\text{int}}^{b} = \frac{1}{2}\langle u_n \rangle \left[K_b^b + K_b^s\right] \{u_n\} \tag{64}$$

Shear Energy :

$$\Pi_{\text{int}}^{s} = \frac{1}{2}\langle u_n \rangle [K_s] \{u_n\} \tag{65}$$

Axial-Bending Coupling Energy:

$$\Pi_{\text{int}}^{ab} = \frac{1}{2}\langle u_n \rangle [K_{ab}] \{u_n\} \tag{66}$$

Axial-Shear Coupling Energy:

$$\Pi_{\text{int}}^{as} = \frac{1}{2}\langle u_n \rangle [K_{as}] \{u_n\} \tag{67}$$

Bending-Shear Coupling Energy:

$$\Pi_{\text{int}}^{bs} = \frac{1}{2}\langle u_n \rangle [K_{bs}] \{u_n\} \tag{68}$$

From above formulation Eq. (63) to Eq. (68), calculations are made and obtained axial stiffness, bending stiffness, shear stiffness and coupling stiffness, respectively:

Global Stiffness : $$[K] = [K_a] + \left[K_b^b\right] + \left[K_b^s\right] + [K_s] + [K_{as}] + [K_{ab}] + [K_{bs}] \tag{69}$$

In Eq. (69), indexes *a, b, s, as, ab,* and *bs* contribute axial, bending, shear, coupling axial-shear, coupling axial-bending and coupling bending-shear respectively to the element stiffness matrix.

The component of axial stiffness element can be expressed by:

$$[K_a] = D_a \int_0^L \{B_a\} \langle B_a \rangle dx; \tag{70}$$

Shear Stiffness element

$$\left[K_s\right] = D_s \int_0^L \{\gamma\}\langle\gamma\rangle \, dx; \quad (71)$$

Bending Stiffness Element

$$\left[K_b^b\right] = D_{bb} \int_0^L \{B_b\}\langle B_b\rangle \, dx \quad (72)$$

$$\left[K_b^s\right] = D_{ss} \int_0^L \{B_s\}\langle B_s\rangle \, dx; \quad (73)$$

Axial Bending Coupling Stiffness element:

$$\left[K_{ab}\right] = -D_{ab} \int_0^L \left\{B_{u_a}\right\}\langle B_b\rangle \, dx - D_{ab} \int_0^L \{B_b\}\left\langle B_{u_a}\right\rangle dx; \quad (74)$$

Axial Shear Coupling Stiffness element:

$$\left[K_{as}\right] = -D_{as} \int_0^L \left\{B_{u_a}\right\}\langle B_s\rangle \, dx - D_{as} \int_0^L \{B_s\}\left\langle B_{u_a}\right\rangle dx; \quad (75)$$

Bending Shear Coupling Stiffness element:

$$\left[K_{bs}\right] = D_{bs} \int_0^L \{B_b\}\langle B_s\rangle \, dx + D_{bs} \int_0^L \{B_s\}\langle B_b\rangle \, dx; \quad (76)$$

And the global stiffness FGM is as follows:

$$K=\begin{bmatrix}
\frac{D_a}{L} & 0 & -\frac{D_{ab}}{L} & 0 & -\frac{D_{as}}{L} & -\frac{D_a}{L} & 0 & \frac{D_{ab}}{L} & 0 & \frac{D_{as}}{L}\\
0 & \frac{12D_{bb}}{L^3} & \frac{6D_{bb}}{L^2} & \frac{12D_{bs}}{L^3} & \frac{6D_{bs}}{L^2} & 0 & -\frac{12D_{bb}}{L^3} & \frac{6D_{bb}}{L^2} & -\frac{12D_{bs}}{L^3} & \frac{6D_{bs}}{L^2}\\
-\frac{D_{ab}}{L} & \frac{6D_{bb}}{L^2} & \frac{4D_{bb}}{L} & \frac{6D_{bs}}{L^2} & \frac{4D_{bs}}{L} & \frac{D_{ab}}{L} & -\frac{6D_{bb}}{L^2} & \frac{2D_{bb}}{L} & -\frac{6D_{bs}}{L^2} & \frac{2D_{bs}}{L}\\
0 & \frac{12D_{bs}}{L^3} & \frac{6D_{bs}}{L^2} & \frac{6D_s}{5L}+\frac{12D_{ss}}{L^3} & \frac{D_s}{10}+\frac{6D_{ss}}{L^2} & 0 & -\frac{12D_{bs}}{L^3} & \frac{6D_{bs}}{L^2} & -\frac{6D_s}{5L}-\frac{12D_{ss}}{L^3} & \frac{D_s}{10}+\frac{6D_{ss}}{L^2}\\
-\frac{D_{as}}{L} & \frac{6D_{bs}}{L^2} & \frac{4D_{bs}}{L} & \frac{D_s}{10}+\frac{6D_{ss}}{L^2} & \frac{4D_{ss}}{L}+\frac{2D_sL}{15} & \frac{D_{as}}{L} & -\frac{6D_{bs}}{L^2} & \frac{2D_{bs}}{L} & -\frac{D_s}{10}-\frac{6D_{ss}}{L^2} & \frac{2D_{ss}}{L}-\frac{D_sL}{30}\\
-\frac{D_a}{L} & 0 & \frac{D_{ab}}{L} & 0 & \frac{D_{as}}{L} & \frac{D_a}{L} & 0 & -\frac{D_{ab}}{L} & 0 & -\frac{D_{as}}{L}\\
0 & -\frac{12D_{bb}}{L^3} & -\frac{6D_{bb}}{L^2} & -\frac{12D_{bs}}{L^3} & -\frac{6D_{bs}}{L^2} & 0 & \frac{12D_{bb}}{L^3} & -\frac{6D_{bb}}{L^2} & \frac{12D_{bs}}{L^3} & -\frac{6D_{bs}}{L^2}\\
\frac{D_{ab}}{L} & \frac{6D_{bb}}{L^2} & \frac{2D_{bb}}{L} & \frac{6D_{bs}}{L^2} & \frac{2D_{bs}}{L} & -\frac{D_{ab}}{L} & -\frac{6D_{bb}}{L^2} & \frac{4D_{bb}}{L} & -\frac{6D_{bs}}{L^2} & \frac{4D_{bs}}{L}\\
0 & -\frac{12D_{bs}}{L^3} & -\frac{6D_{bs}}{L^2} & -\frac{6D_s}{5L}-\frac{12D_{ss}}{L^3} & -\frac{D_s}{10}-\frac{6D_{ss}}{L^2} & 0 & \frac{12D_{bs}}{L^3} & -\frac{6D_{bs}}{L^2} & \frac{6D_s}{5L}+\frac{12D_{ss}}{L^3} & -\frac{D_s}{10}-\frac{6D_{ss}}{L^2}\\
\frac{D_{as}}{L} & \frac{6D_{bs}}{L^2} & \frac{2D_{bs}}{L} & \frac{D_s}{10}+\frac{6D_{ss}}{L^2} & \frac{2D_{ss}}{L}-\frac{D_sL}{30} & -\frac{D_{as}}{L} & -\frac{6D_{bs}}{L^2} & \frac{4D_{bs}}{L} & -\frac{D_s}{10}-\frac{6D_{ss}}{L^2} & \frac{4D_{ss}}{L}+\frac{2D_sL}{15}
\end{bmatrix} \tag{77}$$

The external energy in implementation with uniformly distributed load f_0 can be expressed:

$$\Pi_{ext}=\langle u_n\rangle\{f_n\} \tag{78}$$

$$\langle f_n\rangle = f_0\int_0^L w(x)dx \tag{79}$$

The equivalent nodal force vector uniformly distributed load is given by:

$$\langle f_n\rangle=\left\langle 0 \quad \frac{Lf_0}{2} \quad \frac{L^2f_0}{12} \quad \frac{Lf_0}{2} \quad \frac{L^2f_0}{12} \quad 0 \quad \frac{Lf_0}{2} \quad -\frac{L^2f_0}{12} \quad \frac{Lf_0}{2} \quad -\frac{L^2f_0}{12}\right\rangle \tag{80}$$

3. Static Analysis Results and Comparison

At this stage, some examples of various boundaries are performed for static analysis. Different boundary condition for these supports is presented in Figure 5. The HOBT [21] method will be compared to FOBT for the formulation validity test.

Hinged-Roll	Clamped-Free	Clamped-Clamped	Clamped-Hinged
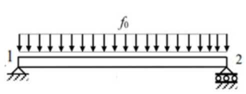	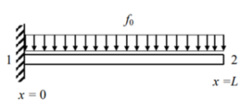	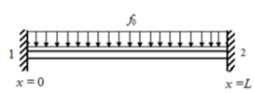	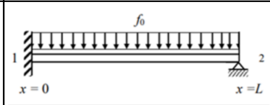
At 1: $u_a=w_b=w_s=0$	**At 1:** $u_a=w_b=w_s=\theta_b=\theta_s=0$	**At 1:** $u_a=w_b=w_s=\theta_b=\theta_s=0$	**At 1=** $u_a=w_b=w_s=\theta_b=\theta_s=0$
At 2: $w_b=w_s=0$		**At 2:** $u_a=w_b=w_s=\theta_b=\theta_s=0$	**At 2=** $u_a=w_b=w_s=0$

Fig. 5. Typical of Beam Support and Boundary Condition

FGM Material Properties to validate the good performance of the HOBT method are as follow:

$E_m = 70GPa$, $v_m = 0.3$ where E_m is the young modulus Aluminium (Al) on the bottom of the beam and $E_c = 200GPa$, $v_c = 0.3$ where E_c is the young modulus of ceramic Zirconia(ZnO2) on top of the beam. Shear correction factor 5/6 is used and, two length-to-height ratios $L/h = 16$ and $L/h = 4$ are applied to the number of powerlaw index (*p=0, 0.2, 0.5, 1, 2, 5,10, ∞*). a uniformly distributed load f_0 are applied.

For convenience, the following dimensionless forms is used:

$$\bar{w} = w\frac{E_m}{f_0 L^4}\frac{h^3}{12}\times 10^3 \quad (81)$$

Table 1 shows that the increasing powerlaw index will increase the deflection. It also represents the convergence of the normalized centre displacements after comparing with UI simplified results. Those results are found similar with the reference [14]. As can be seen in Table 1. the maximum displacements result of hinge-roll support, clamped-free support, clamped–clamped support. and clamped-hinged support of the beam from the proposed element are match with the finite element solutions based on reference [14]. No comparison is shown for HOBT and UI Simplified methods which means the result are reliable. Those two-result different from UI Method [13], UI Method uses 5th Degree Polynomial; therefore, one element is already enough to get exact displacement. UI Simplified and HOBT, which use 3rd Degree Polynomial, need a minimum of 2 elements for a good result, except Clamped-Free supported, which only needs one element to give a good result. However, the present method (HOBT) is a faster formulation than the other two and simpler boundary condition formulation.

Table 1
Non-Dimensional deflections of FGM Beams (Al/) ZnO2) under uniform load

L/h	Reference	NELT	*p* = 0	*p* = 0.2	*p* = 0.5	*p* = 1	*p* = 2	*p* = 5	*p* = 10	*p* = ∞
	Hinge-Roll									
16	FOBT Vo	16	4.6017	5.3559	6.3005	7.3826	8.3962	9.2750	10.0266	13.1471
	UI Simplified	16	4.6017	5.3559	6.3005	7.3826	8.3962	9.2750	10.0266	13.1478
	UI Method	16	4.6017	5.3559	6.3005	7.3826	8.3962	9.2750	10.0266	13.1478
	HOBT	16	4.6017	5.3557	6.3005	7.3810	8.3940	9.2733	10.0266	13.1478
4	FOBT Vo	16	5.2682	6.1034	7.1514	8.3699	9.5724	10.7293	11.6559	15.0521
	UI Simplified	16	5.2682	6.1034	7.1514	8.3699	9.5724	10.7293	11.6559	15.0521
	UI Method	16	5.2682	6.1034	7.1514	8.3699	9.5724	10.7293	11.6559	15.0521
	HOBT	16	5.2682	6.1032	7.1514	8.3684	9.5702	10.7270	11.6559	15.0521
Clamped-Free										
16	FOBT Vo	16	43.9275	51.1375	60.1714	70.5050	80.1675	88.5001	95.6475	125.5075
	UI Simplified	16	43.9275	51.1375	60.1714	70.5050	80.1675	88.5001	95.6475	125.5075
	UI Method	16	43.9275	51.1375	60.1714	70.5050	80.1675	88.5001	95.6475	125.5075
	HOBT	16	43.9280	51.1375	60.1714	70.4990	80.1580	88.4920	95.6475	125.5100
4	FOBT Vo	16	46.5938	54.1275	63.5748	74.4550	84.8713	94.3163	102.1650	133.1250
	UI Simplified	16	46.5938	54.1275	63.5748	74.4550	84.8713	94.3163	102.1650	133.1250
	UI Method	16	46.5938	54.1275	63.5748	74.4550	84.8713	94.3163	102.1650	133.1250
	HOBT	16	46.5938	54.1275	63.5748	74.4490	84.8630	94.3090	102.1600	133.1300
Clamped-Clamped										
16	FOBT Vo	16	0.9559	1.1110	1.3049	1.5289	1.7416	1.9323	2.0921	2.7311
	UI Simplified	16	0.9559	1.1110	1.3049	1.5289	1.7416	1.9323	2.0921	2.7311

	UI Method	16	0.9559	1.1110	1.3049	1.5289	1.7416	1.9323	2.0921	2.7311
	HOBT	16	0.9559	1.1110	1.3049	1.5278	1.7394	1.9323	2.0921	2.7311
4	FOBT Vo	16	1.6224	1.8585	2.1558	2.5164	2.9178	3.3865	3.7213	4.6354
	UI Simplified	16	1.6224	1.8585	2.1558	2.5164	2.9178	3.3865	3.7213	4.6354
	UI Method	16	1.6224	1.8585	2.1558	2.5164	2.9178	3.3865	3.7213	4.6354
	HOBT	16	1.6224	1.8585	2.1558	2.5164	2.9156	3.3865	3.7213	4.6354
Clamped-Hinged										
16	FOBT Vo	16	1.8757	2.1788	2.5519	2.9723	3.3706	3.7477	4.0754	5.3590
	UI Simplified	16	1.8757	2.1788	2.5519	2.9723	3.3706	3.7477	4.0754	5.3590
	UI Method	16	1.8757	2.1788	2.5519	2.9723	3.3706	3.7477	4.0754	5.3590
	HOBT	16	1.8674	2.1688	2.5410	2.9617	3.3703	3.7409	4.0555	5.3339
4	FOBT Vo	16	2.6610	3.0591	3.5518	4.1288	4.7446	5.4494	5.9873	7.6027
	UI Simplified	16	2.6610	3.0591	3.5518	4.1288	4.7446	5.4494	5.9873	7.6027
	UI Method	16	2.6610	3.0591	3.5518	4.1288	4.7446	5.4494	5.9873	7.6027
	HOBT	16	2.5339	2.9170	3.3567	4.1288	4.7446	5.2829	5.7643	7.5180

4. Conclusions

The comparison studies verify the good performance of the Higher Order Beam Theories. The displacement fields of the proposed theories are chosen based on the assumption of two unlinking displacements (bending displacement and shear displacement) through the depth of the beam with 3^{rd}degree polynomial approximation. Equations of motion are derived from Hamilton's energy principle. Numerical Solution are conducted for various types supported beams. The following points can be outlined from the present study:

i. The proposed beam theory gives a high specific stiffness formulation. It satisfies the stress-free boundary conditions on the top and bottom surfaces of the beam and gives convergence results for displacement.
ii. Euler Bernoulli bending is a special case and this present formulation will be free from shear locking. This proposed method could be implemented both thick and thin beam cases.
iii. The results are reliable because the proposed beam theories are match with the others method results and agree well with the existing solutions.
iv. The unlinking shear displacement gives good results for total displacement contribution.

Acknowledgement
The first author gratefully acknowledges Indonesia Endowment Fund for Education (Lembaga Pengelola Dana Pendidikan) Republic Indonesia for granting the scholarship, and the corresponding author thanks to Universitas Indonesia's financial support through the Seed Funding Professor FTUI program.

References
[1] Bui, Xuan-Bach, Trung-Kien Nguyen, Ngoc-Duong Nguyen, and Thuc P. Vo. "A general higher-order shear deformation theory for buckling and free vibration analysis of laminated thin-walled composite I-beams." *Composite Structures* 295 (2022): 115775. https://doi.org/10.1016/j.compstruct.2022.115775
[2] Nguyen, Trung-Kien, Ba-Duy Nguyen, Thuc P. Vo, and Huu-Tai Thai. "A novel unified model for laminated composite beams." *Composite Structures* 238 (2020): 111943. https://doi.org/10.1016/j.compstruct.2020.111943
[3] Nguyen, Trung-Kien, T. Truong-Phong Nguyen, Thuc P. Vo, and Huu-Tai Thai. "Vibration and buckling analysis of functionally graded sandwich beams by a new higher-order shear deformation theory." *Composites Part B: Engineering* 76 (2015): 273-285. https://doi.org/10.1016/j.compositesb.2015.02.032

[4] Timoshenko, Stephen P. "LXVI. On the correction for shear of the differential equation for transverse vibrations of prismatic bars." *The London, Edinburgh, and Dublin Philosophical Magazine and Journal of Science* 41, no. 245 (1921): 744-746. https://doi.org/10.1080/14786442108636264
[5] Timoshenko, Stephan P. "X. On the transverse vibrations of bars of uniform cross-section." *The London, Edinburgh, and Dublin Philosophical Magazine and Journal of Science* 43, no. 253 (1922): 125-131. https://doi.org/10.1080/14786442208633855
[6] Zienkiewicz, O. C., R. L. Taylor, and JM0253 Too. "Reduced integration technique in general analysis of plates and shells." *International Journal for Numerical Methods in Engineering* 3, no. 2 (1971): 275-290. https://doi.org/10.1002/nme.1620030211
[7] Li, X-F. "A unified approach for analyzing static and dynamic behaviors of functionally graded Timoshenko and Euler–Bernoulli beams." *Journal of Sound and vibration* 318, no. 4-5 (2008): 1210-1229. https://doi.org/10.1016/j.jsv.2008.04.056
[8] Kiendl, J., Ferdinando Auricchio, Thomas JR Hughes, and A33103151423 Reali. "Single-variable formulations and isogeometric discretizations for shear deformable beams." *Computer Methods in Applied Mechanics and Engineering* 284 (2015): 988-1004. https://doi.org/10.1016/j.cma.2014.11.011
[9] Falsone, Giovanni, and Dario Settineri. "An Euler–Bernoulli-like finite element method for Timoshenko beams." *Mechanics Research Communications* 38, no. 1 (2011): 12-16. https://doi.org/10.1016/j.mechrescom.2010.10.009
[10] Katili, Irwan. "Unified and integrated approach in a new Timoshenko beam element." *European Journal of Computational Mechanics* 26, no. 3 (2017): 282-308. https://doi.org/10.1080/17797179.2017.1328643
[11] Katili, Irwan. "Metode elemen hingga untuk skeletal." (2004).
[12] Katili, Andi Makarim, and Irwan Katili. "Fea versus iga in a two-node beam element based on unified and integrated method." *Adv. Appl. Math. Mech* 12, no. 6 (2020): 1565-1586. https://doi.org/10.4208/aamm.OA-2018-0255
[13] Katili, Irwan, Tito Syahril, and Andi Makarim Katili. "Static and free vibration analysis of FGM beam based on unified and integrated of Timoshenko's theory." *Composite Structures* 242 (2020): 112130. https://doi.org/10.1016/j.compstruct.2020.112130
[14] Katili, Andi Makarim, and Irwan Katili. "A simplified UI element using third-order Hermitian displacement field for static and free vibration analysis of FGM beam." *Composite Structures* 250 (2020): 112565. https://doi.org/10.1016/j.compstruct.2020.112565
[15] Bui, Xuan-Bach, Trung-Kien Nguyen, Ngoc-Duong Nguyen, and Thuc P. Vo. "A general higher-order shear deformation theory for buckling and free vibration analysis of laminated thin-walled composite I-beams." *Composite Structures* 295 (2022): 115775. https://doi.org/10.1016/j.compstruct.2022.115775
[16] Nguyen, Trung-Kien, T. Truong-Phong Nguyen, Thuc P. Vo, and Huu-Tai Thai. "Vibration and buckling analysis of functionally graded sandwich beams by a new higher-order shear deformation theory." *Composites Part B: Engineering* 76 (2015): 273-285. https://doi.org/10.1016/j.compositesb.2015.02.032
[17] Ma, Haitao. "Rational approach for higher-order shear deformation beam theories." *Composite Structures* 251 (2020): 112599. https://doi.org/10.1016/j.compstruct.2020.112599
[18] Carrera, Erasmo, and Marco Petrolo. "On the effectiveness of higher-order terms in refined beam theories." (2011): 021013. https://doi.org/10.1115/1.4002207
[19] Li, Xian-Fang, Bao-Lin Wang, and Jie-Cai Han. "A higher-order theory for static and dynamic analyses of functionally graded beams." *Archive of Applied Mechanics* 80 (2010): 1197-1212. https://doi.org/10.1007/s00419-010-0435-6
[20] Kadoli, Ravikiran, Kashif Akhtar, and N. Ganesan. "Static analysis of functionally graded beams using higher order shear deformation theory." *Applied mathematical modelling* 32, no. 12 (2008): 2509-2525. https://doi.org/10.1016/j.apm.2007.09.015
[21] Thai, Huu-Tai, and Thuc P. Vo. "Bending and free vibration of functionally graded beams using various higher-order shear deformation beam theories." *International journal of mechanical sciences* 62, no. 1 (2012): 57-66. https://doi.org/10.1016/j.ijmecsci.2012.05.014
[22] Vinayak, R. U., G. Prathap, and B. P. Naganarayana. "Beam elements based on a higher order theory—I. Formulation and analysis of performance." *Computers & structures* 58, no. 4 (1996): 775-789. https://doi.org/10.1016/0045-7949(95)00185-J
[23] Thai, Huu-Tai, and Thuc P. Vo. "Bending and free vibration of functionally graded beams using various higher-order shear deformation beam theories." *International journal of mechanical sciences* 62, no. 1 (2012): 57-66. https://doi.org/10.1016/j.ijmecsci.2012.05.014
[24] Kadoli, Ravikiran, Kashif Akhtar, and N. Ganesan. "Static analysis of functionally graded beams using higher order shear deformation theory." *Applied mathematical modelling* 32, no. 12 (2008): 2509-2525. https://doi.org/10.1016/j.apm.2007.09.015

[25] Reddy, Junuthula N. "A simple higher-order theory for laminated composite plates." (1984): 745-752. https://doi.org/10.1115/1.3167719

[26] Wang, C. M., Junuthula Narasimha Reddy, and K. H. Lee, eds. *Shear deformable beams and plates: Relationships with classical solutions*. Elsevier, 2000.

[27] Yesilce, Yusuf, and Seval Catal. "Free vibration of axially loaded Reddy-Bickford beam on elastic soil using the differential transform method." *Struct. Eng. Mech* 31, no. 4 (2009): 453-476. https://doi.org/10.12989/sem.2009.31.4.453

[28] Yesilce, Yusuf. "Effect of axial force on the free vibration of reddy—bickford multi-span beam carrying multiple spring—mass systems." *Journal of Vibration and Control* 16, no. 1 (2010): 11-32. https://doi.org/10.1177/1077546309102673

[29] Yesilce, Yusuf, and Hikmet H. Catal. "Solution of free vibration equations of semi-rigid connected Reddy–Bickford beams resting on elastic soil using the differential transform method." *Archive of Applied Mechanics* 81 (2011): 199-213. https://doi.org/10.1007/s00419-010-0405-z

[30] Vo, Thuc P., Huu-Tai Thai, Trung-Kien Nguyen, and Fawad Inam. "Static and vibration analysis of functionally graded beams using refined shear deformation theory." *Meccanica* 49 (2014): 155-168. https://doi.org/10.1007/s11012-013-9780-1